Analysis of Technology Improvement Opportunities for a 1.5 MW Wind Turbine using a Hybrid Stochastic Approach in Life Cycle Assessment

Matthew Ozoemena[1], Reaz Hasan [2] *, Wai Ming Cheung[3]

[1, 2, 3] Dept. of Mechanical & Construction Engineering, Northumbria University, Newcastle Upon Tyne, NE1 8ST, UK

*corresponding author: reaz.hasan@northumbria.ac.uk

Abstract: This paper presents an analysis of potential technological advancements for a 1.5 MW wind turbine using a hybrid stochastic method to improve uncertainty estimates of embodied energy and embodied carbon. The analysis is specifically aimed at these two quantities due to the fact that LCA based design decision making is of utmost importance at the concept design stage. In the presented case studies, better results for the baseline turbine were observed compared to turbines with the proposed technological advancements. Embodied carbon and embodied energy results for the baseline turbine show that there is about 85% probability that the turbine manufacturers may have lost the chance to reduce carbon emissions, and 50% probability that they may have lost the chance to reduce the primary energy consumed during its manufacture. The paper also highlights that the adopted methodology can be used to support design decision making and hence is more feasible for LCA studies.

Keywords: Embodied energy; Embodied carbon; Technology Improvement Opportunities; Uncertainty; LCA; 1.5 MW wind turbine

List of symbols and abbreviations

LCA	Life Cycle Assessment
EEC	Embodied energy coefficient
EF	Emission Factor
DQI	Data Quality Indicator
HDS	Hybrid Data Quality Indicator and Statistical
MCS	Monte Carlo Simulation
K-S	Kolmogorov-Smirnov
MRE	Mean Magnitude of Relative Error
M_{HDS}	Mean of HDS result
M_{DQI}	Mean of DQI result

CV	Coefficient of Variation
σ	Standard deviation
μ	Mean
N_M	Least number of data points required
N_{MD}	Least number of required data points for individual parameter distribution estimation
N_P	Number of parameters involved
NREL	National Renewable Energy Laboratory
MW	Megawatt
TIO	Technology Improvement Opportunities
CFRP	Carbon Fibre Reinforced Plastic
PDF	Probability distribution function
CDF	Cumulative distribution function

1.0 Introduction

The development of efficient and cleaner energy technologies and the use of renewable and new energy sources will play a significant role in the sustainable development of a future energy strategy (Ghenai, 2012; Weitemeyer et al., 2015). It is highlighted in International Energy Agency (2013) that the development of cleaner and more efficient energy systems and promotion of renewable energy sources are a high priority for (i) economic and social cohesion, (ii) diversification and security of energy supply and (iii) environmental protection. Electricity generation using wind turbines is generally regarded as key in addressing some of the resource and environmental concerns of today. According to the World Wind Energy Association (2014), wind energy technology has steadily improved and costs have declined. This technological progress is obvious in the movement to better wind conditions and shift to higher nominal power of wind turbines (Wang and Sun, 2012; Weinzettel et al., 2009). However, all renewable systems for converting energy into usable forms such as electricity have environmental impacts associated with them (Davidsson et al., 2012; Kelly et al., 2014) and is an important issue in mainstream debate. Further, as pointed out by Chen et al. (2011) and Yang et al. (2013), it is essential that the long term sustainability of such systems are scrutinized to support the astonishing growth (actual plus planned) of wind farms as well as to allow policy makers to take robust decisions to mitigate climate change through the implementation of this technology at the design stage.

The production of renewable energy sources, like every other production process, involves the consumption of natural resources and energy as well as the release of pollutants (Ardente et al., 2008). Life cycle assessment (LCA) is a popular way of measuring the energy performance and environmental impacts of wind energy (Davidsson et al., 2012; Martínez et al., 2010). Hammond and Jones (2008) defined embodied energy of a material as the total amount of primary energy consumed over its life cycle. This would normally encompass extraction, manufacturing and transportation and the terminology has been in use for over four decades (Constanza, 1980). In a similar fashion embodied carbon refers to the lifecycle greenhouse gas emissions (expressed as carbon dioxide equivalents – CO_2e) that occur during the manufacture and transport of a material. Embodied energy and embodied carbon assessments are considered a subset of LCA studies.

The production of renewable energy sources, like every other production process, involves the consumption of natural resources and energy as well as the release of pollutants (Ardente et al., 2008). Life cycle assessment (LCA) is a popular way of measuring the energy performance and environmental impacts of wind energy (Davidsson et al., 2012; Martínez et al., 2010). Hammond and Jones (2008) defined embodied energy of a material as the total amount of primary energy consumed over its life cycle. This would normally encompass extraction, manufacturing and transportation and the terminology has been in use for over four decades (Constanza, 1980). In a similar fashion embodied carbon refers to the lifecycle greenhouse gas emissions (expressed as carbon dioxide equivalents – CO_2e) that occur during the manufacture and transport of a material (Chen et al., 2011). Embodied energy and embodied carbon assessments are considered a subset of LCA studies.

Embodied energy and embodied carbon are traditionally estimated deterministically using single fixed point input values to generate single fixed point results (Lloyd and Ries, 2007). Lack of detailed production data and differences in production processes result in substantial variations in emission factor (EF) and embodied energy coefficient (EEC) values among different life cycle inventory (LCI) databases (Sugiyama et al., 2005; Wang and Shen, 2013). Hammond and Jones (2008) notes that a comparison of selected values in these inventories would show a lot of similarities but also several differences. These variations termed as “data uncertainty” in Huijbregts (1998) significantly affect the results of embodied energy and embodied carbon LCA studies. Uncertainty is unfortunately part of embodied carbon and energy analysis and even data that is very reliable carries a natural level of uncertainty (Kabir et al., 2012; Hammond and Jones, 2008). Hence, the analysis of data uncertainty is a significant improvement to the deterministic approach because it provides more information for decision making (Wang and Shen, 2013; Kabir et al., 2012; Sugiyama et al., 2005; Tan et al., 2002).

A number of generally accepted and well understood methods such as stochastic modelling, analytical uncertainty propagation, interval calculations, fuzzy data sets and scenario modelling are normally used to propagate uncertainty in LCA analysis. In a survey of approaches used to incorporate uncertainty in LCA studies, Lloyd and Ries (2007) have found that the majority of the published work employed scenario modelling to propagate uncertainty on LCA outcomes (Martínez et al., 2010; Guezuraga et al., 2012; Greening and Azapagic, 2013; Demir and Taşkın, 2013; Tremeac and Meunier, 2009; Zhong et al., 2011; Uddin and Kumar, 2014; Garrett and Rønde, 2013; Zimmermann, 2013; Padey et al., 2012; Oebels and Pacca, 2013; Martínez et al., 2009; Aso and Cheung, 2015), while only three (Kabir et al., 2012; Fleck and Huot, 2009; Khan et al., 2005), have employed stochastic modelling to propagate uncertainty. Of the twelve studies using scenario modelling, all assessed scenarios using sensitivity analysis, while for the studies employing stochastic modelling, all used Monte Carlo simulation with random sampling. The Monte Carlo analysis method used by Kabir et al. (2012), Fleck and Huot (2009) and Khan et al. (2005) performs well for cases when reliability of the uncertainty estimate is not of utmost importance. This method has a drawback when applied, as due to its "rule of thumb" nature it may lead to inaccurate results. For more reliable results, Lloyd and Ries (2007) highlights that the determination of significant contributors to uncertainty, selection of appropriate distributions and maintaining correlation between parameters are areas requiring better understanding.

In this study, a methodology (termed as HDS) for improving uncertainty estimate is presented and discussed. The method employs the same basics as the Monte Carlo analysis but has a key distinction, aiming at removing the drawback of the Monte Carlo analysis method by employing a stochastic pre-screening process to determine the influence of parameter contributions. The very reliable statistical method is then used to estimate probability distributions for the identified critical parameters. By applying the HDS method to a baseline 1.5 MW wind turbine and four Technology Improvement Opportunity variants (Cohen et al., 2008; Lantz et al., 2012), the uncertainty estimates of embodied energy and embodied carbon are examined. This methodology can be a very valuable tool for making informed decisions at the design stage in order to make savings on embodied energy and embodied carbon by taking into consideration the uncertainty estimates of these quantities. The overall aim of this study is to present an analysis of potential technological advancements for a 1.5 MW wind turbine using a hybrid stochastic method to improve uncertainty estimates of embodied energy and embodied carbon. The organisation of the content of this paper is as follows: Section 2 explains the fundamentals of the methodology. Section 3 contains a description of the case studies and their background theory. In Section 4 the results are analysed and discussed. Finally, in Section 5, conclusion and future work are presented.

2.0 Methodology

Statistical and Data quality indicator (DQI) methods are used to estimate data uncertainty in LCA with different limitations and advantages (Lloyd and Ries, 2007; Wang and Shen, 2013). The statistical method uses a goodness of fit test to fit data samples characterizing data range with probabilistic distributions if sufficient data samples are available (Wang and Shen, 2013). On the other hand, the DQI method estimates data uncertainty and reliability based on expert knowledge and descriptive metadata e.g. source of data, geographical correlation of data etc. It is used quantitatively (Lloyd and Ries, 2007) and qualitatively (Lloyd and Ries, 2007; Junnila and Horvath, 2003). Compared to the statistical method the DQI costs less, although it is less accurate than the statistical method (Wang and Shen, 2013; Tan et al., 2002). The statistical method is preferred when high accuracy is required, though its implementation cost is high (Wang and Shen, 2013; Sugiyama et al., 2005). The DQI method is generally applied when the accuracy of the uncertainty estimate is not paramount, or the size of the data sample is not sufficient enough for significant statistical analysis (Wang and Shen, 2013).

Considering the trade-off between cost of implementation and accuracy, Wang and Shen (2013) presented an alternative stochastic solution using a hybrid DQI-statistical (HDS) approach to reduce the cost of the statistical method while improving the quality of the pure DQI method in whole-building embodied energy LCA. The study focused on the reliability of the HDS approach compared to the pure DQI without considering the effect of either approach on the decision making process. An application test case to the analysis of embodied energy and embodied carbon of potential 1.5 MW wind turbine technological advancements and the effect of these approaches on decision making is presented here to validate the presented solution. A description of the methodology is given below.

2.1 Embodied Energy and Embodied Carbon Estimation

This study considers embodied energy and embodied carbon as the primary environmental impacts to be investigated. Wang and Sun (2012) and Ortiz et al. (2009) express embodied carbon and embodied energy mathematically as follows:

$$Embodied\ Carbon = \sum_{i=1}^{n} Q_i \times EF_i \tag{1}$$

$$Embodied\ Energy = \sum_{i=1}^{n} Q_i \times EEC_i \tag{2}$$

Where

Q_i = Quantity of material *i*

EEC_i = Embodied energy coefficient of material *i*

EF_i = Emission factor of material *i*

Since the purpose of the different wind turbine designs is electricity production, the functional unit is defined as 'generation of 1 KWh of electricity'. The scope of the study for all the wind turbine design options considered is from 'cradle to gate'.

2.2 Qualitative DQI method

Qualitative DQI uses descriptive indicators, often arranged as a Data Quality Indicator (DQI) matrix (Table 1), to characterize data quality. Rows in the matrix represent a quality scale, ranging from 1 to 5 or 1 to 10. Columns represent data quality indicators such as age of the data, reliability of the data source etc. General quality for a data is specified by an aggregated number that takes into account all the indicators. For example if three indicators are assigned scores of (1, 3, 5) respectively for a given parameter, and the indicators are equally weighted, the parameter's aggregated DQI score is P = 1 × 1/3 + 3 × 1/3 + 5 × 1/3 = 3.

	Quality Scale				
Data Quality Indicators	1	2	3	4	5
Data representativeness	Representativeness unknown or incomplete data from insufficient sample of sites and/or for a shorter period	Data from a smaller number of sites for a shorter period, or incomplete data from an adequate number of sites and periods	Representative data from an adequate number of sites but for a shorter period	Representative data from a smaller number of sites but for an adequate period	Representative data from a sufficient sample of sites over an adequate period to even out normal fluctuations
Age	≥15 years old	<15 years old	<10 years old	<6 years old	<3 years old
Acquisition method	Non-qualified estimation	Qualified estimation by experts	Calculated data partly based on assumptions	Calculated data based on measurements	Directly measured data

Supplier independence	Unverified information from enterprise interested in the study	Unverified information from irrelevant enterprise	Independent source but based on unverified information	Verified data from enterprise with interest in the study	Verified data from independent source
Geographical correlation	Unknown area	Data from an area with slightly similar production conditions	Data from an area with similar production conditions	Average data	Data from the exact area
Technological correlation	Data from process related of company with different technology	Data from process related of company with similar technology	Data from process studied of company with different technology	Data from process studied of company with similar technology	Data from process studied of the exact company with the exact technology
Rule of inclusion/ exclusion	Unknown	Non-transparent on exclusion but specification of inclusion	Transparent, not-justified, uneven application	Transparent, justified, uneven application	Transparent, justified, homogeneous application

Table 1: Data Quality Indicator (DQI) matrix based on NETL (2010), Weidema and Wesnæs (1996) and Junnila and Horvath (2003).

2.3 Quantitative DQI method

This method transforms aggregated DQI scores into probability distributions to enable quantification of uncertainty using predefined uncertainty parameters. Data of different quality are characterized by distinct probability distributions that are based on “rule of thumb”. Table 2 shows the DQI transformation matrix usually used to transform aggregated DQI scores into beta functions as shown in Equation (3):

$$f(x;\alpha,\beta,a,b) = \left[\frac{1}{b-a}\right] * \left\{\frac{\Gamma(\alpha+\beta)}{[\Gamma(\alpha) * \Gamma(\beta)]}\right\} * \left[\frac{x-a}{b-a}\right]^{\alpha-1} * \left[\frac{b-x}{b-a}\right]^{\beta-1} \quad (3)$$

$$(a \leq x \leq b)$$

Where α, β are shape parameters of the distribution and a, b are designated range endpoints. The beta function is used due to the fact that “the range of end points and shape parameters allow practically any shape of probability distributions to be represented”.

Aggregated DQI scores	Beta distribution function	
	Shape parameters (α, β)	Range endpoints (+/- %)
5.0	(5, 5)	10
4.5	(4, 4)	15
4.0	(3, 3)	20
3.5	(2, 2)	25
3.0	(1, 1)	30
2.5	(1, 1)	35
2.0	(1, 1)	40
1.5	(1, 1)	45
1.0	(1, 1)	50

Table 2: Transformation matrix based on (Canter et al., 2002 and Weidema and Wesnæs, 1996).

2.4 HDS approach

The HDS approach involves four steps: (i) Quantitative DQI with Monte Carlo simulation (MCS); (ii) Categorization of parameters; (iii) Detailed estimation of probability distributions for parameters; and (iv) Final MCS calculation. The parameter characterization identifies the critical parameters based on the influence and degree of uncertainty of the parameters. The final stochastic results are generated through a MCS calculation.

2.4.1 Quantitative DQI with MCS

This step begins with assessing data quality using the qualitative DQI approach. All parameters used for the deterministic calculations are assessed using the DQI matrix. After calculation of the aggregated DQI scores, probability distributions for the parameters are determined using the transformation matrix (Table 2), and used as inputs for the MCS to carry out an influence analysis.

2.4.2 Categorization of parameters

The degree of parameter uncertainty is obtained in the data quality assessment process. Parameters are consequently classified into groups of four with DQI scores belonging to the intervals of (1, 2), (2, 3), (3, 4) and (4, 5) respectively. The group containing parameters with DQI scores within the interval of (1, 2) and (2, 3) show the highest uncertainty, and the group with parameters scored within the interval of (3, 4) and (4, 5) represent the highest certainty. A parameter's influence on the final resulting uncertainty comes from a rank-order correlation analysis in MCS (Equations (4) and (5)).

$$IA_{p,q} = r_{p,q}^2 \left[\sum_p r_{p,q}^2 \right]^{-1} \times 100\% \tag{4}$$

Where $IA_{p,q}$ is the influence of input parameter p to output q; $r_{p,q}$ is the rank-order correlation factor between input p and the output q. $r_{p,q}$ can be computed via:

$$r_{p,q} = 1 - \left[\frac{6}{(N^3 - N)}\right] \sum_{i=1}^{N} [rank(p_i) - rank(q_i)]^2 \quad (5)$$

Where rank (p_i) and rank (q_i) are the ranks of p_i and q_i among the N tuple data points.

2.4.3 Detailed estimation of probability distributions for parameters

The statistical method is applied to the process of probability distributions fitting for the critical parameters identified. Kolmogorov-Smirnov goodness of fit test (K-S test) is used to fit data samples due to its sensitivity to variations in distribution types in terms of shape and scale parameters, and its intrinsic exactness compared to other goodness of fit tests e.g. Chi-square test and Anderson-Darling (A-D) test. The statistic for the K-S test is defined as:

$$D = \max_{1 \le i \le N} \left[F(Y_i) - \frac{i-1}{N}, \frac{i}{N} - F(Y_i)\right] \quad (6)$$

Where F is the theoretical cumulative distribution of the distribution that is being tested, and N means N ordered data points Y_1, Y_2, …, Y_N.

For the non-critical parameters of lower uncertainty and influence, their probability distributions are estimated using the transformation matrix and the DQI scores, making the HDS approach more economical and efficient compared to the statistical method.

2.4.4 Final MCS calculation

The stochastic results are calculated by MCS algorithm, according to the input and output relationships, using the intricately estimated probability distributions for the parameters' as the inputs. Figure 1 shows the procedure for the HDS approach.

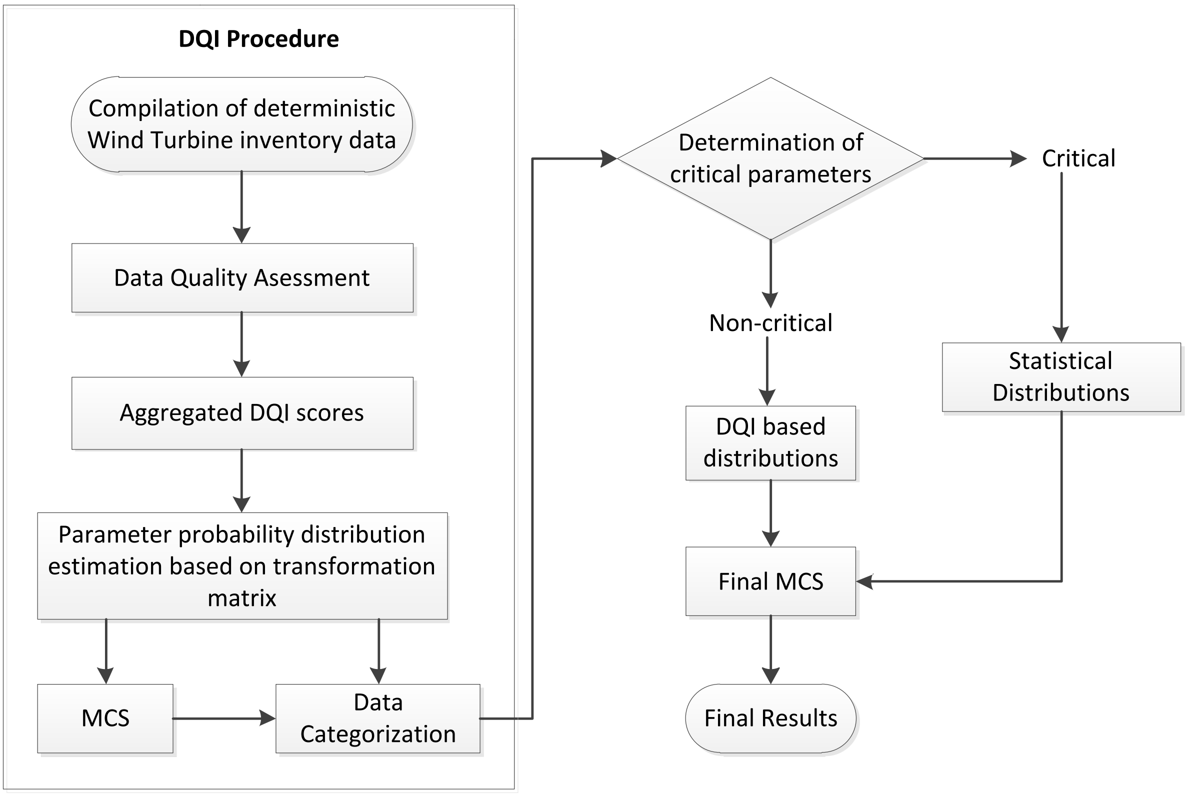

Figure 1: Procedure of HDS approach (Wang and Shen, 2013)

2.5 Validation

To validate the HDS approach, comparisons are made between the pure DQI, statistical and HDS methods. The measurements Mean Magnitude of Relative Error (*MRE*) (Eq. (7)) and Coefficient of Variation (*CV*) (Eq. (8)) are used to measure the differences in the results of the pure DQI and HDS. CV is an indicator that shows the degree of uncertainty and measures the spread of a probability distribution. A large CV value indicates a wide distribution spread. The data requirements are also used to compare the HDS with the statistical method, as large enough sample size needs to be satisfied during parameter distribution estimation. The least number of data points necessary for estimating parameter distributions in each method is calculated (Eq. (9)) and compared.

$$MRE = \frac{(M_{HDS} - M_{DQI})}{M_{HDS}} \times 100\% \quad (7)$$

Where M_{DQI} is the mean of the DQI results and M_{HDS} is the mean of the HDS results

$$CV = \frac{SD}{M} \quad (8)$$

Where *M* is the mean and *SD* is the standard deviation

$$N_M = N_{MD} \times N_P \quad (9)$$

Where N_M is the least number of data points required; N_{MD} is the least number of required data points for individual parameter distribution estimation; N_P is the number of parameters involved.

3.0 Case Studies

Projections of future technological designs as a result of research and scientific developments, based on National Renewable Energy Laboratory (NREL) 1.5 MW wind turbine technology forecasting studies (Cohen et al., 2008 and Lantz et al., 2012), provided the basis for modelling future inventory changes. Therefore, the assumptions regarding a reference from which progress is measured are the embodied energy and embodied carbon characteristics. A summary of the potential for technology advancements to increase the performance of a 1.5 MW wind turbine is presented in the following section.

3.1 Baseline Turbine Characterization

To project advances in reliability and performance of wind turbine systems, a baseline 1.5 MW wind turbine technology must first be identified. This baseline technology will serve as a reference from which performance improvements are projected. The NREL's baseline turbine technology characteristics represent an upwind, variable-pitch, variable-speed, three-bladed turbine that uses a doubly fed generator rated at 1.5 MW. The height of the tower is 65 meters and the rotor diameter is 70 meters. As such, an Enercon E-66 1.5 MW turbine was chosen as it shares similar technical characteristics to the NREL baseline turbine. A technical summary of the Enercon E-66 1.5MW turbine can be seen in Table 3 (Papadopoulos, 2010). The aggregated inventory data, presented in Table 4 (Papadopoulos, 2010), was used for deterministic estimation of embodied energy and embodied carbon. Since the material quantities were taken from the same source, they have little or no variations. The deterministic result estimate (Table 4) is used as a point of reference for comparing outputs of the stochastic estimation.

MODEL:	ENERCON E-66
Rated capacity:	1.5 MW
Rotor diameter:	70 m
Hub height:	65 m
Swept area:	3421 m^2
Converter concept:	gearless, variable speed, variable blade pitch
Rotor with pitch control	upwind rotor with active pitch control
Number of blades:	3
Rotor speed:	variable, 10 -22 rpm
Tip speed:	35 – 76 m/s

Pitch control:	three synchronized blade pitch systems with emergency supply
Generator:	direct-driven ENERCON synchronous ring generator
Grid feeding:	ENERCON inverter
Braking system:	3 independent pitch control systems with emergency supply

Table 3: E-66 technical characteristics (Papadopoulos, 2010)

Components	Materials	Mass (tons)	EF (ton CO_2/ton)	EEC (GJ/ton)	Embodied Carbon (ton CO_2)	Embodied Energy (GJ)
Blades, nacelle	Aluminium	0.2	1.98	155	0.4	31
Blades, nacelle	Fibre glass	7.5	8.1	100	60.8	750
Blades	Epoxy resin	4.5	5.91	139.3	26.6	625.5
Blades	Polyethene	0.7	1.94	83.1	1.4	58.2
Blades, grid connection, foundation	PVC	2.1	2.41	77.2	5.1	162
Blades, tower, generator, nacelle	Paint	5.4	3.56	68	19.2	367.2
Blades	Rubber	0.2	3.18	101.7	0.6	20.3
Blades, grid connection	Iron	1.5	1.91	25	2.9	37.5
Tower	Steel	144.2	2.75	24.4	396.6	3518.5
Tower, generator, nacelle, grid connection	Galvanized steel	6.7	2.82	39	19	261.3
Generator, nacelle, grid connection	Copper	15.4	3.83	50	59	770
Generator, grid connection	Steel sheet	19.2	2.51	31.5	48.2	604.8
Generator, nacelle, foundation	Steel (no alloy)	37.3	1.77	34.4	66	1283
Generator, grid connection	Steel (alloy, high grade)	0.6	2.78	56.7	1.7	34
Nacelle, grid connection	Steel (alloy, low grade)	10	2.68	48.4	26.8	484
Nacelle	Cast Steel	3.7	2.83	25.4	10.5	94
Nacelle	Cast iron	21	1.9	26	40.7	546
Nacelle	Unsaturated polyester resin	2.2	1.94	113	4.2	248.6
Nacelle, grid connection	Electronics	2.5	2.73	80.5	6.8	201.3

Grid connection, foundation	Steel (for construction)	27	0.68	36	18.4	972
Grid connection	Gear oil	0.9	3.62	55	3.3	49.5
Grid connection	Light weight concrete	12	0.13	0.77	1.6	9.24
Foundation	Normal concrete	575	0.2	1.39	115	799.3
	Sum	900.1			932	11910

Table 4: Deterministic estimation of embodied energy and embodied carbon for the Enercon E-66 1.5 MW turbine based on the aggregated inventory data in Papadopoulos (2010)

3.2 Technology Improvement Opportunities (TIOs)

According to Cohen et al. (2008) and Lantz et al. (2012), identification of TIO's relied on judgements and technical insights of the senior research staff at the Sandia National Laboratories and National Wind Technology Centre at the NREL. The design of wind turbines is a matter of continuous compromise between the rival demands of greater energy productivity, lower cost, increased durability and lifetime, and maintenance cost. Realizing greater energy production may cost less or more. These are the designers' trade-offs captured in the model. Trade-offs between wind turbine components is dealt with in the estimation of the input parameters. The outcome of the details of the TIOs is summarized in Table 5.

Performance Improvement	Technology Pathway	Description
TIO 1	Advanced (Enlarged) Rotors	Stiffer carbon-fibre materials allowing for 25% rotor growth and 2% reduction in tower mass
TIO 2	Advanced Tower Concepts	New tower concepts using carbon-fibre materials and power production at 100 meters compared to 65 meters
TIO 3	Drivetrain Improvements	Permanent Magnet Generators that use permanent magnets instead of copper wound rotors
TIO 4	Fully Combined TIO's	A combination of all the potential technological advancements

Table 5: Potential contributions to wind turbine performance improvement

3.3 Mass Scaling Equations

To generate the material quantities for the different TIO's, information and scaling equations were taken from an NREL study (Fingersh et al., 2006). The report contained information about how the various components could be scaled using semi-empirical formulas. The equations used in this study are defined in Table 6 as well as an indication as to where they were employed.

Component	Equation	Description
Blade	$Baseline: Mass = 0.1452 \times R^{2.9158}\ per\ blade$ $Advanced: Mass = 0.4948 \times R^{2.53}\ per\ blade$	Where R = rotor radius. The advanced blade mass relationship follows products developed by a wind turbine blade manufacturer which "represents combinations of technology enhancements that may not/may include carbon and takes advantage of a lower-weight root design".
Tower	$Baseline: Mass = 0.3973 \times \text{swept area} \times \text{hub height} - 1414$ $Advanced: Mass = 0.2694 \times \text{swept area} \times \text{hub height} + 1779$	The baseline case is based on conventional technology for 2002, while the advanced case represents advanced technologies including reduced blade solidity in conjunction with higher tip speeds, flap-twist coupling in the blade and tower feedback in the control system.
Generator	$Mass = 5.34 \times machine\ rating^{0.9223}$	A generator mass calculation for the medium-speed permanent-magnet generator design was based on machine power rating in kW.

Table 6: Mass scaling equations for the different components

4.0 Results and Analysis

4.1 Quantitative DQI transformation

To appropriately transform the qualitative assessment results to the equivalent quantitative probability density functions, Wang and Shen (2013) suggests that the aggregated DQI scores be approximated to the nearest nominal value so as to use the transformation matrix. Figure 2 shows the obtained aggregated DQI scores following the method described in section 2.1. The quantitative DQI procedure was then used to transform the scores into Beta distributions, results of which are shown in Table 7. Most of the data used in the study are of good quality and hence showed identical transformed Beta function parameters (α = 4, β = 4), the same DQI score of 4.5 and range end points of ± 15%. The exceptions were Cast iron EF, Cast iron EEC and Gear oil EEC showing DQI scores of 3.5, transformed Beta function parameters of (α = 2, β = 2) and range end points of ± 25% making them more uncertain.

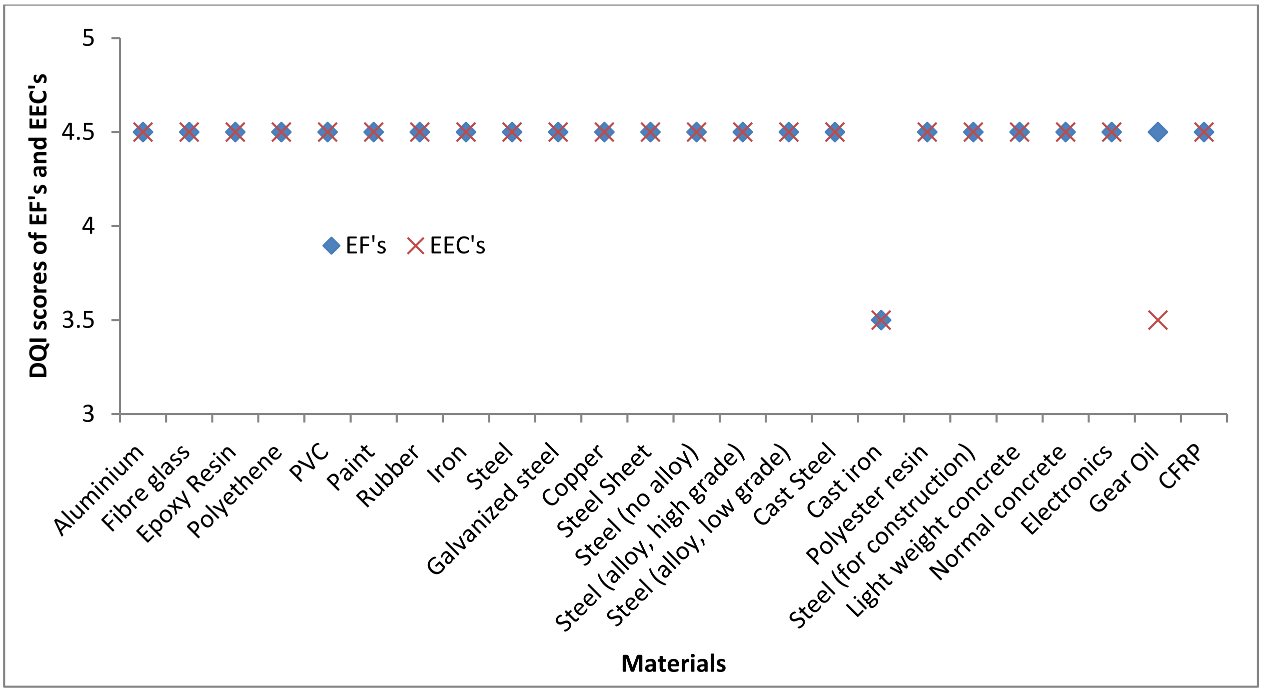

Figure 2: Aggregated DQI scores for Emission Factors and Embodied Energy Coefficients

EF Parameters	Beta (α, β)	Range endpoints	EEC Parameters	Beta (α, β)	Range endpoints
Aluminium (EF)	(4, 4)	(+/-15%) = (1.7, 2.3)	Aluminium (EEC)	(4, 4)	(+/-15%) = (131.8, 178.3)
Fibre glass (EF)	(4, 4)	(+/-15%) = (6.9, 9.3)	Fibre glass (EEC)	(4, 4)	(+/-15%) = (85, 115)
Epoxy resin (EF)	(4, 4)	(+/-15%) = (5, 6.8)	Epoxy resin (EEC)	(4, 4)	(+/-15%) = (118, 160)
Polyethene (EF)	(4, 4)	(+/-15%) = (1.7, 2.2)	Polyethene (EEC)	(4, 4)	(+/-15%) = (70.6, 95.6)
PVC (EF)	(4, 4)	(+/-15%) = (2.1, 2.8)	PVC (EEC)	(4, 4)	(+/-15%) = (65.6, 88.8)
Paint (EF)	(4, 4)	(+/-15%) = (3, 4.1)	Paint (EEC)	(4, 4)	(+/-15%) = (57.8, 78.2)
Rubber (EF)	(4, 4)	(+/-15%) = (2.7, 3.7)	Rubber (EEC)	(4, 4)	(+/-15%) = (86.4, 117)
Iron (EF)	(4, 4)	(+/-15%) = (1.6, 2.2)	Iron (EEC)	(4, 4)	(+/-15%) = (21.3, 28.8)
Steel (EF)	(4, 4)	(+/-15%) = (2.3, 3.2)	Steel (EEC)	(4, 4)	(+/-15%) = (20.7, 28)

Galvanized steel (EF)	(4, 4)	(+/-15%) = (2.4, 3.2)	Galvanized steel (EEC)	(4, 4)	(+/-15%) = (33.2, 45)
Copper (EF)	(4, 4)	(+/-15%) = (3.3, 4.4)	Copper (EEC)	(4, 4)	(+/-15%) = (42.5, 57.5)
Steel sheet (EF)	(4, 4)	(+/-15%) = (2.1, 2.9)	Steel sheet (EEC)	(4, 4)	(+/-15%) = (27, 36.2)
Steel (no alloy) (EF)	(4, 4)	(+/-15%) = (1.5, 2)	Steel (no alloy) (EEC)	(4, 4)	(+/-15%) = (29.2, 39.6)
Steel (alloy, high grade) (EF)	(4, 4)	(+/-15%) = (2.4, 3.2)	Steel (alloy, high grade) (EEC)	(4, 4)	(+/-15%) = (48.2, 65.2)
Steel (alloy, low grade) (EF)	(4, 4)	(+/-15%) = (2.3, 3.1)	Steel (alloy, low grade) (EEC)	(4, 4)	(+/-15%) = (41, 55.7)
Cast Steel (EF)	(4, 4)	(+/-15%) = (2.4, 3.3)	Cast Steel (EEC)	(4, 4)	(+/-15%) = (21.6, 29.2)
Cast iron (EF)	(2, 2)	(+/-25%) = (1.4, 2.4)	Cast iron (EEC)	(2, 2)	(+/-25%) = (19.5, 32.5)
Unsaturated polyester resin (EF)	(4, 4)	(+/-15%) = (1.7, 2.2)	Unsaturated polyester resin (EEC)	(4, 4)	(+/-15%) = (96.1, 130)
Electronics (EF)	(4, 4)	(+/-15%) = (2.3, 3.1)	Electronics (EEC)	(4, 4)	(+/-15%) = (68.4, 92.6)
Steel (for construction) (EF)	(4, 4)	(+/-15%) = (0.6, 0.8)	Steel (for construction) (EEC)	(4, 4)	(+/-15%) = (30.6, 41.4)
Gear oil (EF)	(4, 4)	(+/-15%) = (3.1, 4.2)	Gear oil (EEC)	(2, 2)	(+/-25%) = (41.3, 69)
Light weight concrete (EF)	(4, 4)	(+/-15%) = (0.1, 0.2)	Light weight concrete (EEC)	(4, 4)	(+/-15%) = (0.7, 0.9)
Normal concrete (EF)	(4, 4)	(+/-15%) = (0.2, 0.2)	Normal concrete (EEC)	(4, 4)	(+/-15%) = (1.2, 1.6)

Table 7: Transformation of DQI scores to probability density functions

4.2 Parameter Categorization and Probability Distributions Estimation

Results of the influence analysis (10,000 iterations MCS) showing the two parameters contributing the most to the resulting uncertainty is presented in Table 8. Two parameters, Steel and CFRP, demonstrated the largest influence on the final resulting uncertainty of embodied energy and embodied carbon across all case studies. For the parameters with a lesser contribution to the final resulting uncertainty, there were variations across all case studies. Normal concrete and Carbon fibre reinforced plastic (CFRP) show the lesser contribution for embodied carbon (ranging from 0.6% to 17%), while Steel (no alloy), CFRP and Cast iron show the lesser contribution for embodied energy (ranging from 0.5% to 9%) across all case studies. Combining these results, further analysis was conducted on the two identified parameters for each test case using the statistical method, while the values for the remaining parameters were obtained from the quantitative DQI. Probability distributions were thus fitted to data points collected manually from literature. Results of the estimated probability distributions for the different parameters are presented in Table 9.

	Embodied Carbon	Influence (%)	Embodied Energy	Influence (%)
Baseline	Steel EF	78	Steel EEC	62
Turbine	Normal concrete EF	9	Steel (no alloy) EEC	9
TIO 1	Steel EF	66	Steel EEC	47
	CFRP EF	17	CFRP EEC	22
TIO 2	CFRP EF	99	CFRP EEC	97
	Normal concrete EF	0.3	Steel (no alloy) EEC	0.7
TIO 3	Steel EF	81	Steel EEC	66
	Normal concrete EF	8	Cast iron EEC	9
TIO 4	CFRP EF	98	CFRP EEC	97
	Normal concrete EF	0.6	Steel (no alloy) EEC	0.5

Table 8: Influence Analysis

Parameter	Probability Distribution	Mean	Data points collected	Source
Steel EF	Beta (1.2, 4.5)	1.7 $tonCO_2/ton$	30	Hammond and Jones, 2008; Fleck and Huot, 2009; Alcorn and Wood, 1998; Norgate et al., 2007; Rankine et al., 2006; Khan et al., 2005; Change, 2006; Hammond and Jones, 2011; Lee et al., 2011; Baird et al., 1997
Steel EEC	Beta (3, 4.2)	25.9 GJ/ton	31	
Normal concrete EF	Beta (20.8, 87.7)	0.1 $tonCO_2/ton$	31	Hammond and Jones, 2008; Hammond and Jones, 2011; Alcorn and Wood, 1998; Norgate et al., 2007; Rankine et al., 2006
Steel (no alloy) EEC	Beta (48.6, 62.3)	25.6 GJ/ton	31	Hammond and Jones, 2008; Alcorn and Wood, 1998; Norgate et al., 2007; Rankine et al., 2006; Khan et al., 2005; Change, 2006; Lee et al., 2011; Baird et al., 1997; Fernando, 2010
CFRP EF	Beta (3.2, 2.2)	52.4 $tonCO_2/ton$	31	Hill et al., 2011; Kirihara et al., 2011; Pimenta and Pinho, 2011; Howarth et al., 2014; Douglas et al., 2008; Song et al., 2009; Rydh and Sun, 2005; Duflou et al., 2012
CFRP EEC	Beta (2.1, 6.2)	191.3 GJ/ton	31	
Cast iron EEC	Beta (36.6, 75.2)	35.4 GJ/ton	31	Fernando, 2010; Du et al., 2012; TERI, 2012; Hendrickson and

	Horvath, 2014; Sharma et al., 2013; Baum et al., 2009; Sefeedpari et al., 2012; Lenzen and Dey, 2000; Lenzen and Treloar, 2002; Baird et al., 1997

Table 9: Probability distribution estimation for the different parameters

4.3 Stochastic Results Comparison of DQI and HDS Approaches for the Different Case Studies

Embodied carbon and embodied energy stochastic results (10,000 iterations MCS) using the pure DQI and HDS methods were obtained for the baseline turbine and TIO's 1 - 4 the results of which are presented in this section. Results for each case study are presented graphically through probability distribution functions (PDF's) and cumulative distribution functions (CDF's) in Figures 3 – 12. In addition to these figures, MRE and CV values were also calculated. A summary of the relevant information is provided in Table 10.

	Embodied Carbon		Embodied Energy	
	DQI	HDS	DQI	HDS
Baseline Turbine	Beta distribution (4.5, 5.3) μ = 932 tonCO_2 σ = 22 tonCO_2 CV = 0.02	Beta distribution (1.8, 5.1) μ = 733 tonCO_2 σ = 183 tonCO_2 CV = 0.3 MRE = 27%	Normal distribution μ = 11909 GJ σ =218 GJ CV = 0.02	Beta distribution (4.4, 4.7) μ = 11831 GJ σ = 1424 GJ CV = 0.1 MRE = 1%
TIO 1	Normal distribution μ =1070 tonCO_2 σ = 24 tonCO_2 CV = 0.02	Beta distribution (2.3, 5.2) μ =1269 tonCO_2 σ =188 tonCO_2 CV = 0.2 MRE = 16%	Normal distribution μ = 13735 GJ σ = 244 GJ CV = 0.02	Beta distribution (3.8, 4.7) μ = 13276 GJ σ = 1469 GJ CV = 0.1 MRE = 3.5%
TIO 2	Beta distribution (5, 5.3) μ = 2475 tonCO_2 σ = 96 tonCO_2 CV = 0.04	Beta distribution (5.8, 4.1) μ = 5521 tonCO_2 σ = 1654 tonCO_2 CV = 0.3 MRE = 55%	Beta distribution (4.1, 4.8) μ = 31822 GJ σ = 1166 GJ CV = 0.04	Beta distribution (2.4, 4.7) μ =24687 GJ σ = 7608 GJ CV = 0.3 MRE = 29%
TIO 3	Beta distribution (5.3, 5.7) μ = 849 tonCO_2 σ = 22 tonCO_2 CV = 0.03	Beta distribution (1.6, 4.6) μ = 647 tonCO_2 σ =185 tonCO_2 CV = 0.3	Normal distribution μ =10722 GJ σ =211 GJ CV = 0.02	Beta distribution (3.8, 4.8) μ =11249 GJ σ = 1474 GJ CV = 0.1

		MRE = 31%		MRE = 5%
TIO 4	Gamma distribution (529, 4.8) μ = 2529 $tonCO_2$ σ = 108 $tonCO_2$ CV = 0.04	Weibull distribution (4, 6621) μ = 5988 $tonCO_2$ σ = 1746 $tonCO_2$ CV = 0.3 MRE = 58%	Beta distribution (4.7, 4.5) μ = 32503 GJ σ = 1304 GJ CV = 0.04	Beta distribution (2.1, 4.6) μ = 24299 GJ σ = 8419 GJ CV = 0.4 MRE = 33%

Table 10: Pure DQI and HDS results for the different case studies

Probability distributions were fitted to the stochastic results according to K-S test. From the PDF's (Figures 3a – 12a), it can be seen that the mean value and standard deviation for the pure DQI and HDS results show rather different dispersion across all the case studies. The CV values of the HDS results are on average about 6 times larger than the CV values of the pure DQI results. In terms of MRE, the difference observed between the HDS and pure DQI results indicate that the HDS method captures more possible outcomes compared to the pure DQI. The differences between the deterministic, pure DQI and HDS results can be inferred from the CDF's (Figures 3b – 12b). Figure 3b for example shows that for the HDS result, about 85% of the likely resulting values are smaller than the deterministic result obtained while for the DQI result, 50% of the possible results are smaller than the deterministic result. Figure 5b also shows that for the HDS result about 15% of the likely results are smaller than the deterministic result while for the DQI result, half of the possible resulting values are lesser than the deterministic result. A comprehensive analysis of the implications of these results is presented in the discussion section.

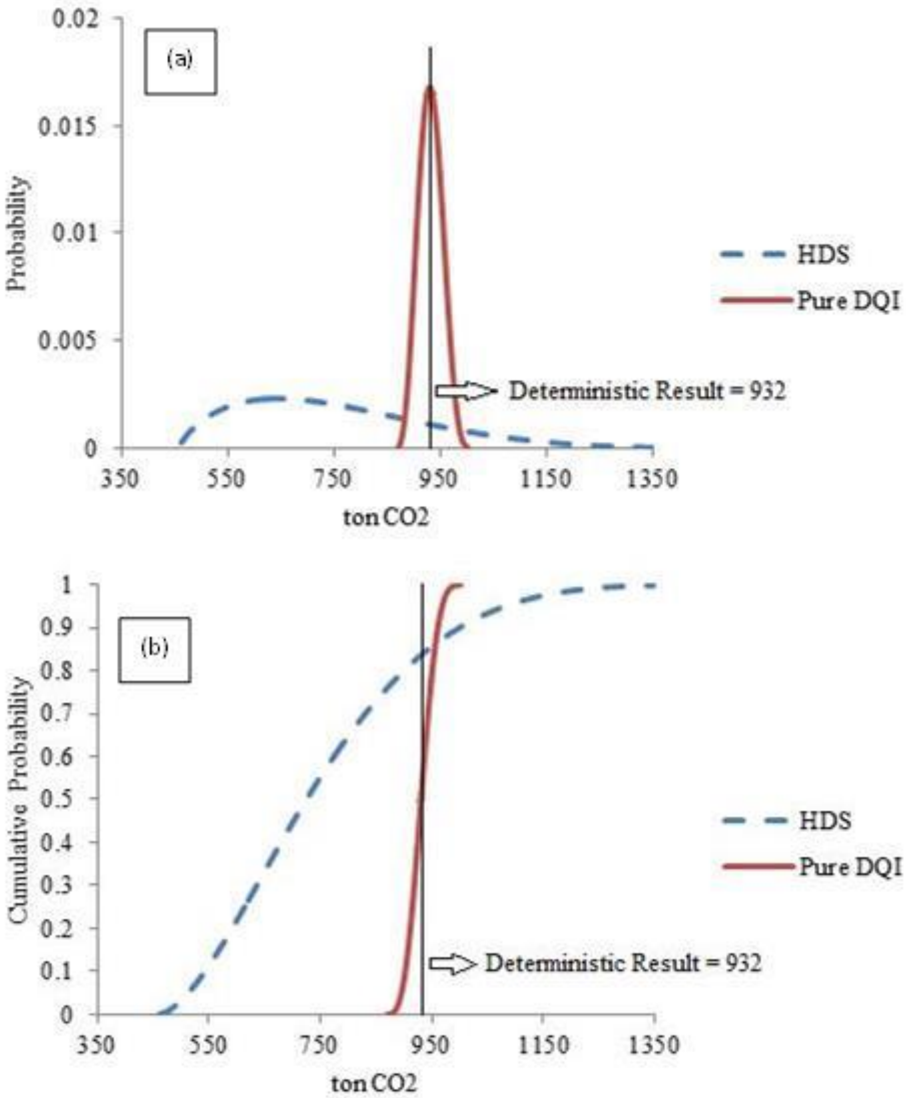

Figure 3 (a) Baseline Turbine Embodied Carbon PDF results; (b) Baseline Turbine Embodied Carbon CDF results

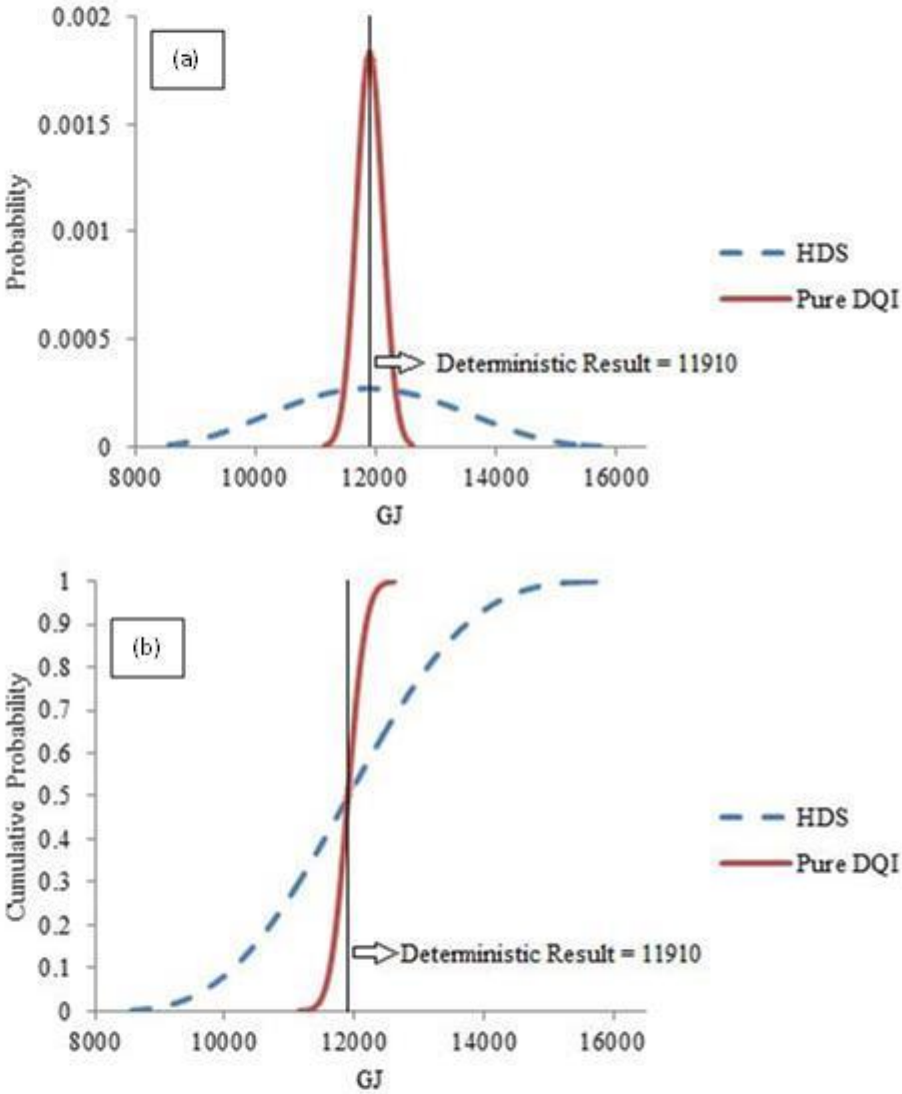

Figure 4 (a) Baseline Turbine Embodied Energy PDF results; (b) Baseline Turbine Embodied Energy CDF results

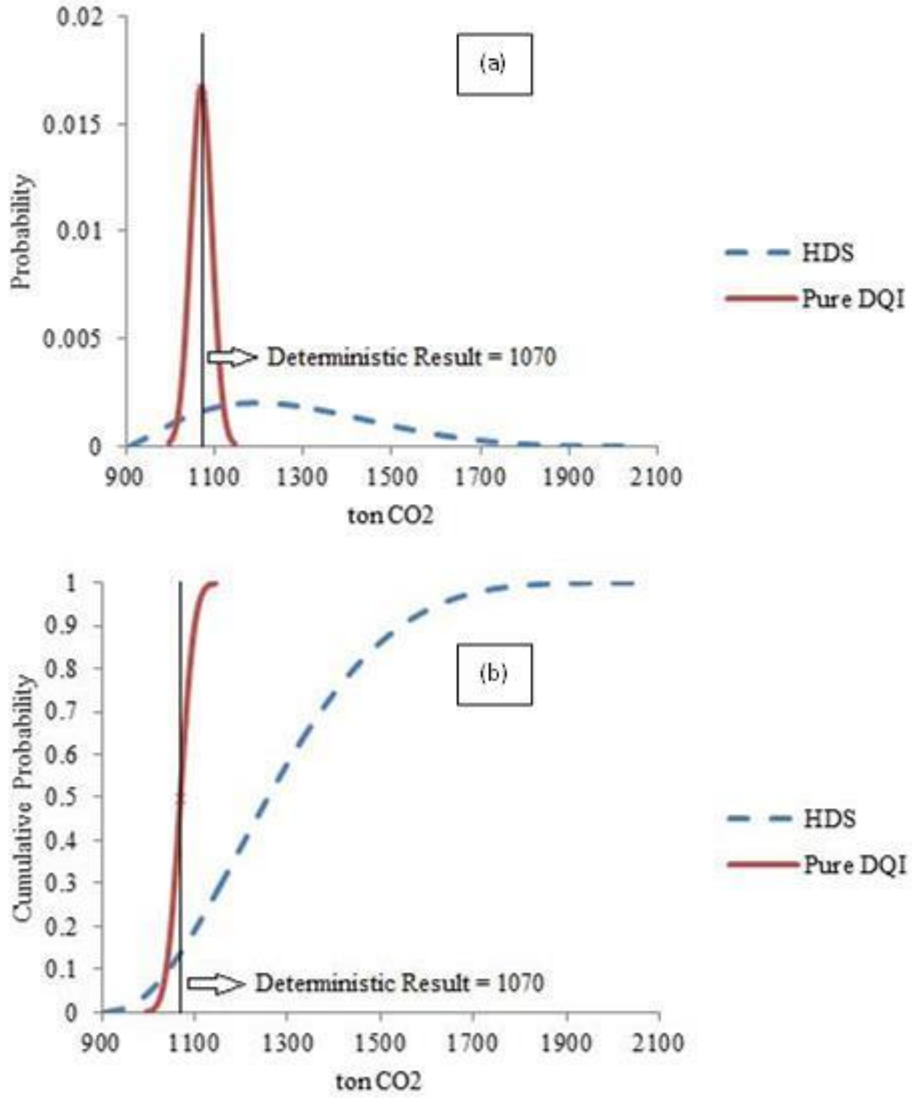

Figure 5 (a) TIO 1 Embodied Carbon PDF results; (b) TIO 1 Embodied Carbon CDF results

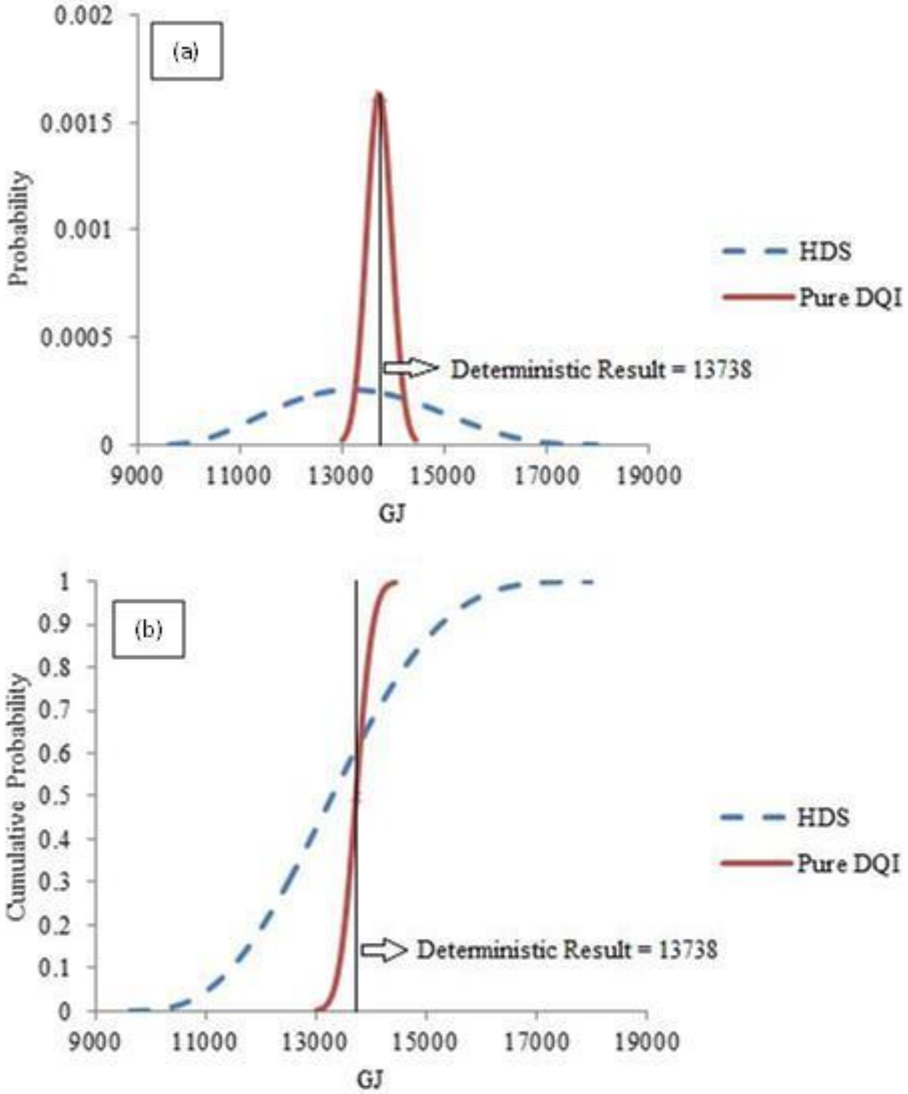

Figure 6 (a) TIO 1 Embodied Energy PDF results; (b) TIO 1 Embodied Energy CDF results

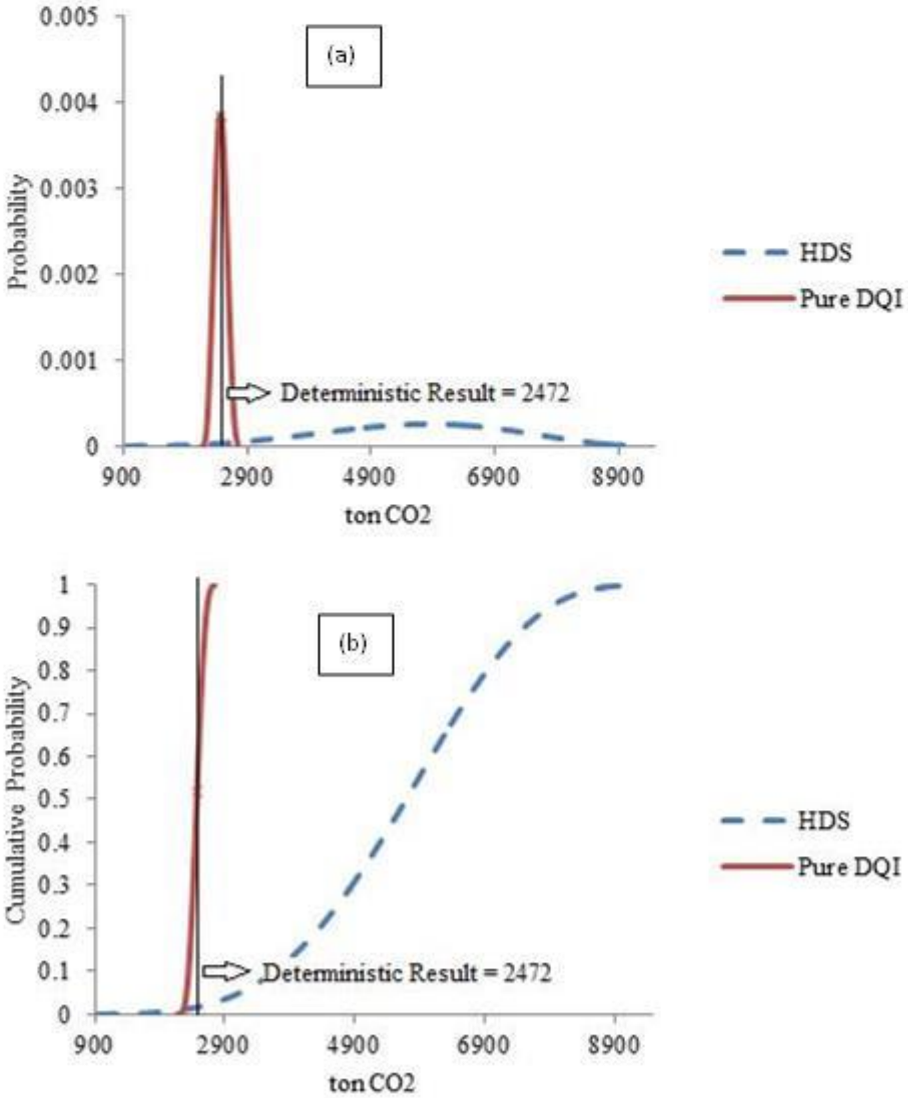

Figure 7 (a) TIO 2 Embodied Carbon PDF results; (b) TIO 2 Embodied Carbon CDF results

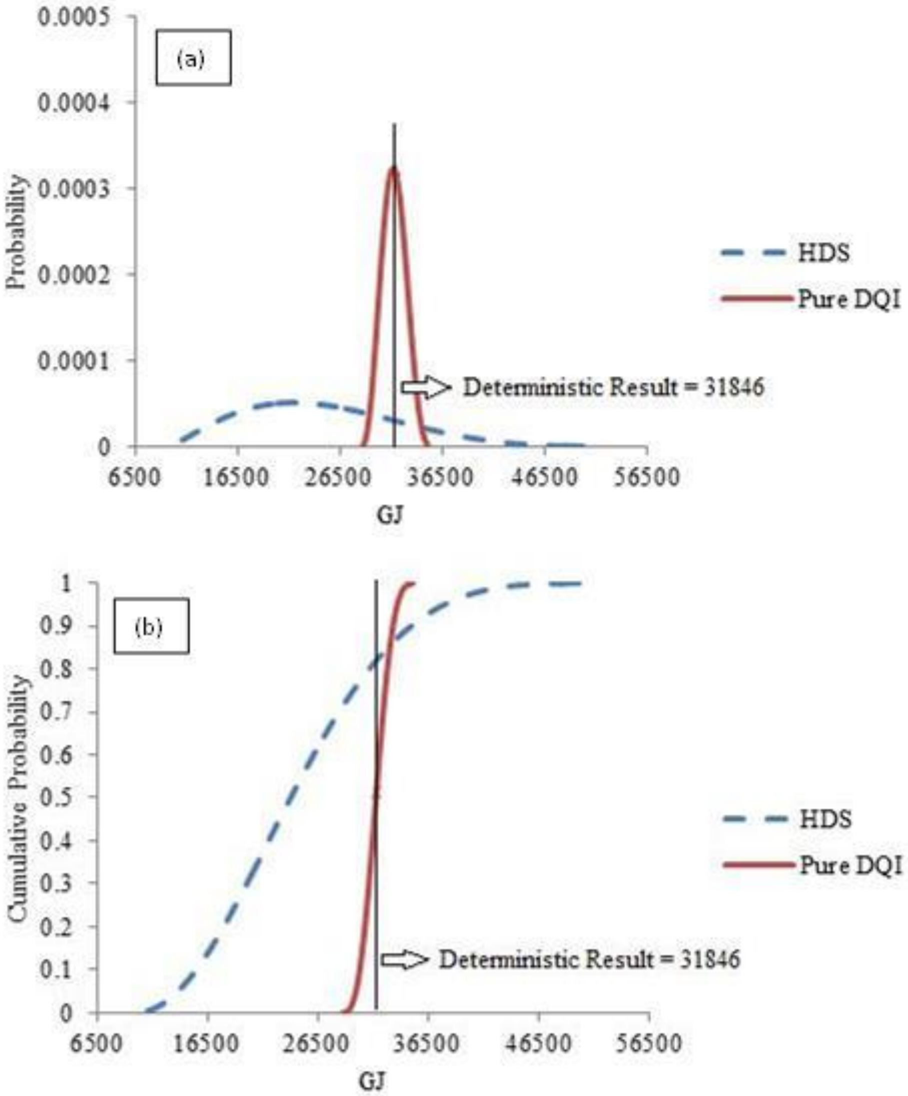

Figure 8 (a) TIO 2 Embodied Energy PDF results; (b) TIO 2 Embodied Energy CDF results

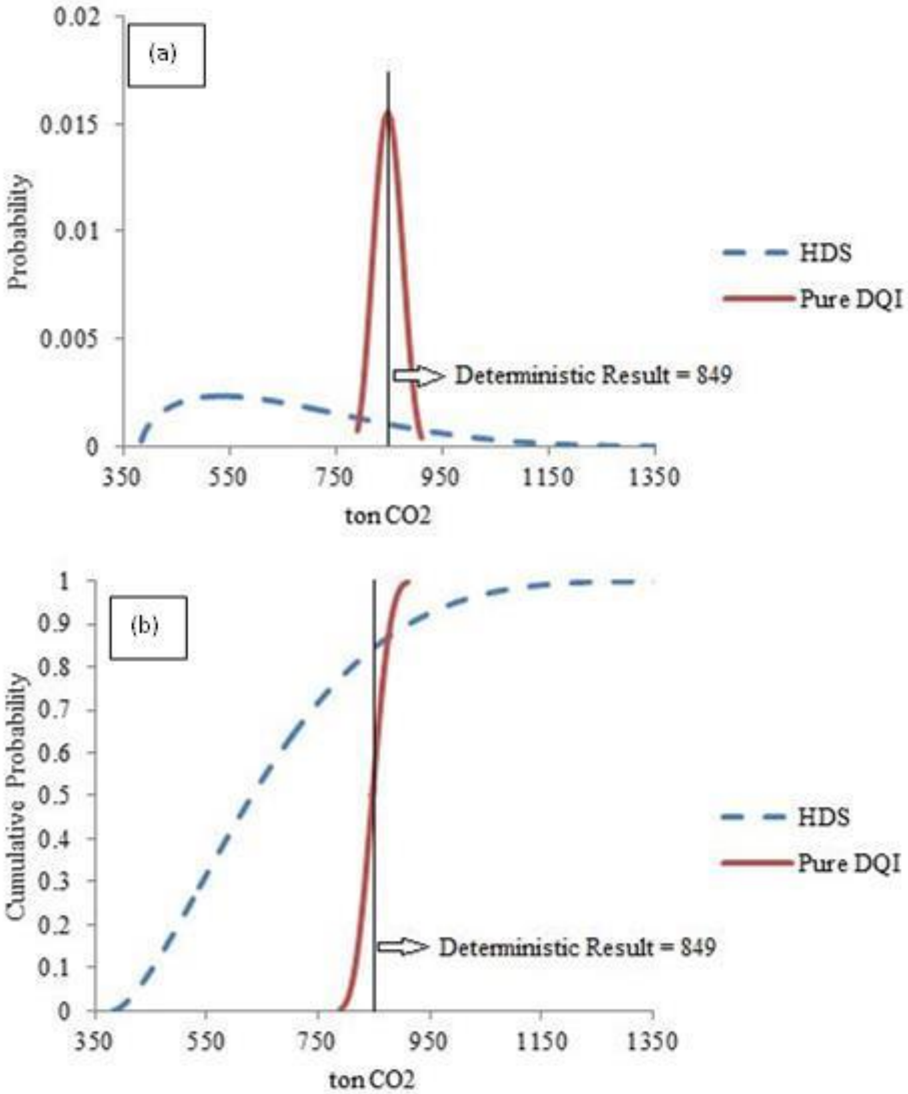

Figure 9 (a) TIO 3 Embodied Carbon PDF results; (b) TIO 3 Embodied Carbon CDF results

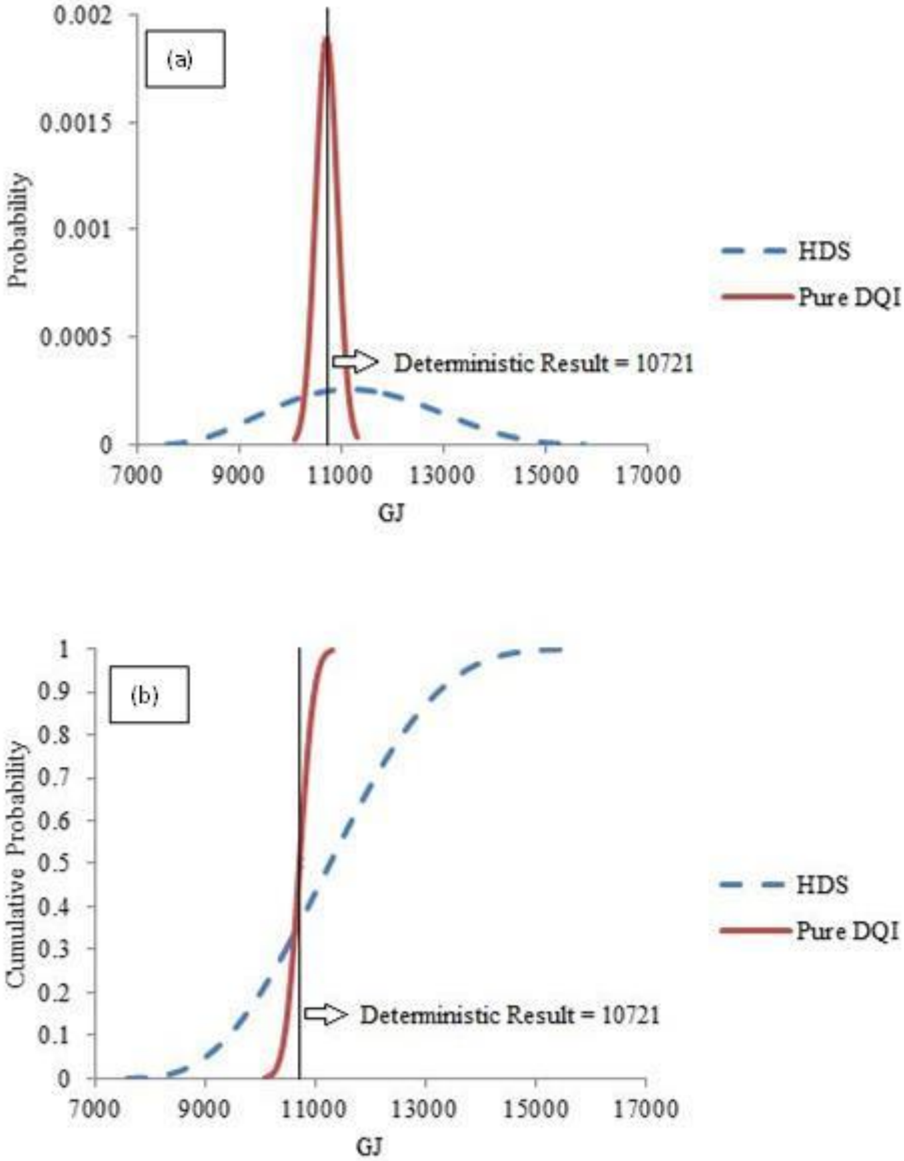

Figure 10 (a) TIO 3 Embodied Energy PDF results; (b) TIO 3 Embodied Energy CDF results

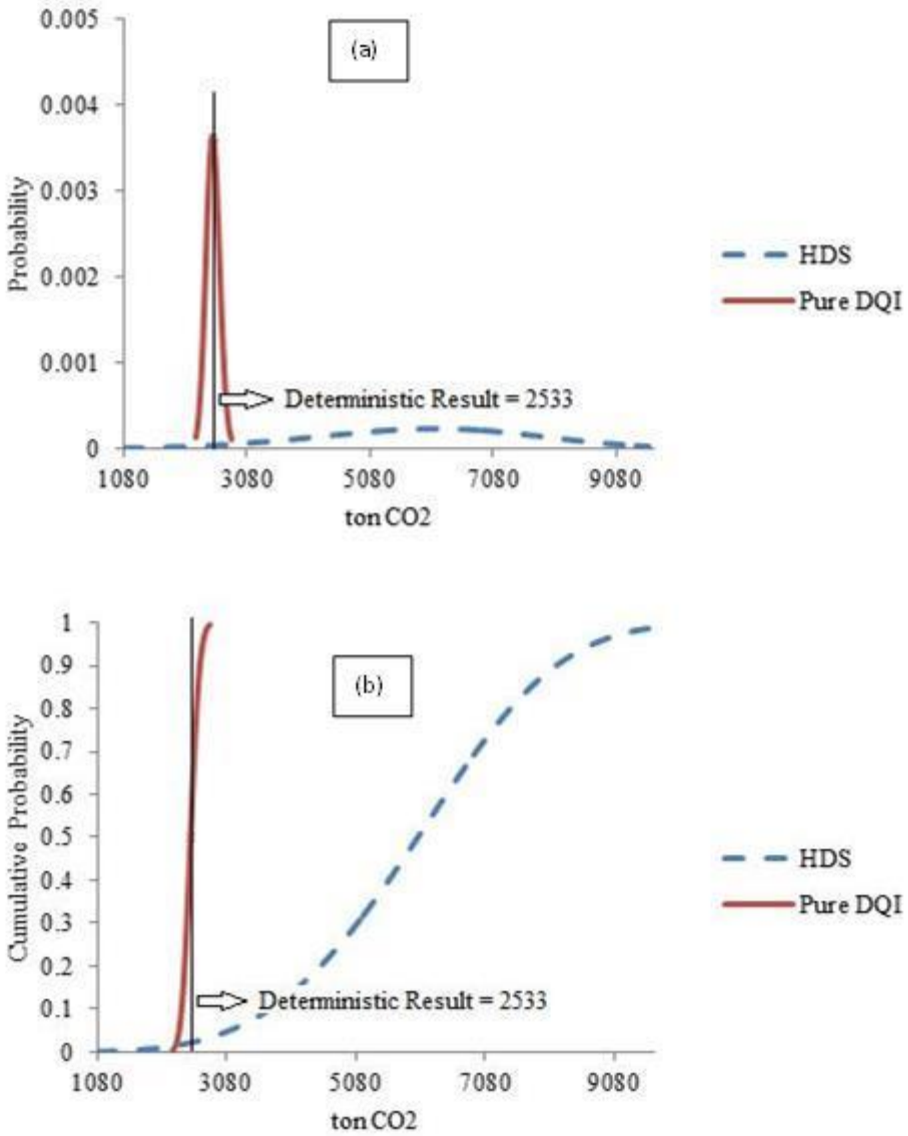

Figure 11 (a) TIO 4 Embodied Carbon PDF results; (b) TIO 4 Embodied Carbon CDF results

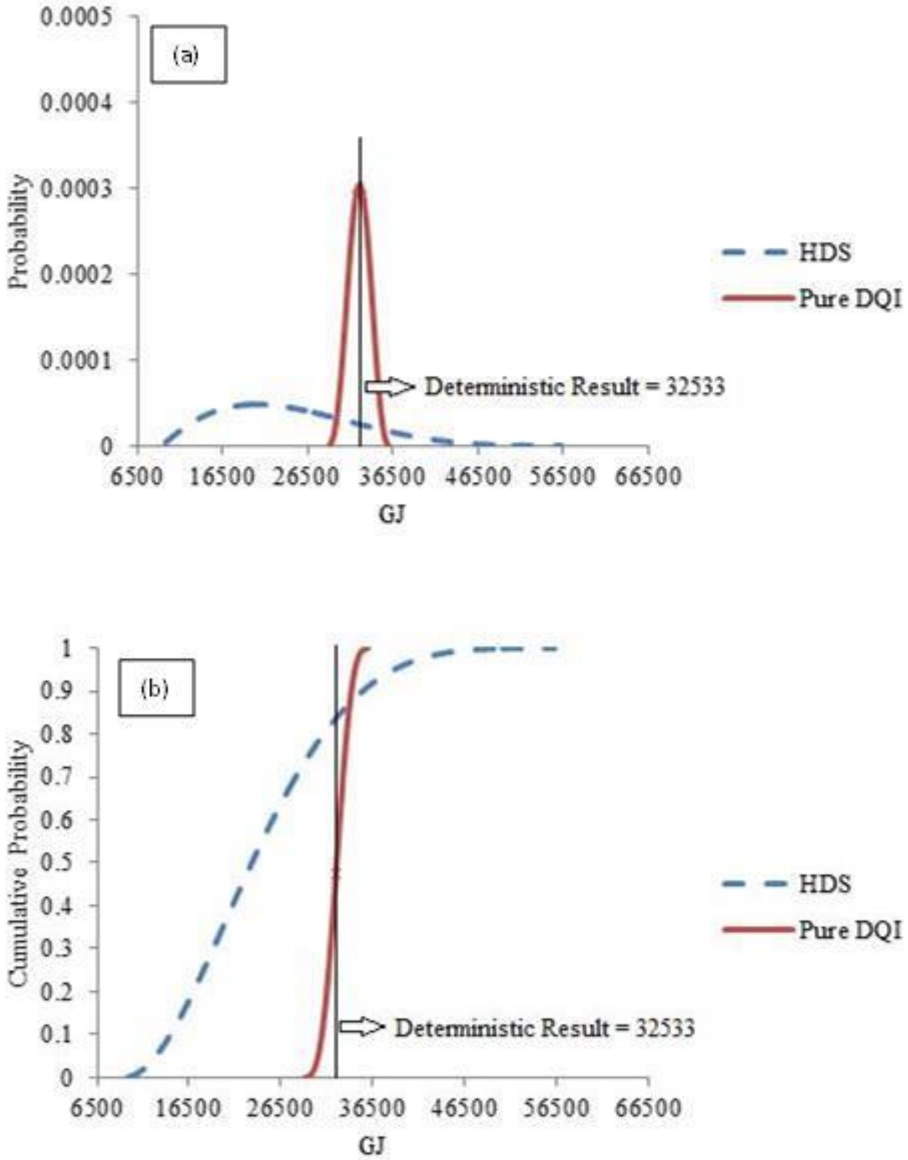

Figure 12 (a) TIO 4 Embodied Energy PDF results; (b) TIO 4 Embodied Energy CDF results

4.4 Comparison of Statistical and HDS Methods in terms of Data Requirements

It can be seen that from the procedure of the HDS approach which categorizes critical parameters and uses the statistical method to estimate their probability distributions, the reliability of the HDS results are not greatly jeopardized. According to Wang and Shen (2013), the statistical method requires at least 30 data points to estimate one parameter distribution. Hence in this study, 46 parameter distributions are required to be estimated for each case study with the exception of TIO 1 which has 48 parameter distributions for estimation. If the statistical method was implemented, at least 1380 (see Equation 9) data points would have been required for the estimation for each case study. That would mean 6900 data points across all the case studies. This would have been very time consuming even if all the data points were available. The HDS requires only 120 data points for each case study (600 data points across all the case studies) thus reducing the data requirements by approximately 91%. This avoids the issue associated with lack of data, and saves cost and time without seriously compromising the reliability of the HDS results as the critical parameters identified explain the majority (at least 69%) of the overall uncertainty across all the case studies.

4.5 Discussion

This study uses the HDS approach to provide insight into potential technological advancements for a 1.5 MW wind turbine and makes evident how variability of input parameters results in differing embodied energy and embodied carbon results. Analysing the parameter categorization revealed that EF's and EEC's for Steel, Normal concrete, Steel (no alloy), CFRP and Cast iron accounted for the majority of output uncertainty in embodied energy and embodied carbon results. Steel is the main material component of the baseline wind turbine, followed by normal concrete. The large contribution of steel is probably attributed to the wide EF and EEC distributions assigned to steel in the probability distribution estimations. Therefore any uncertainty in steel EF's and EEC's is magnified by the sheer mass of steel. Interestingly although the mass of concrete (575 tons) is greater than the mass of steel (144 tons), steel EF's and EEC's contribute more to the overall uncertainty of embodied energy and embodied carbon. For example, the EF's of steel ranges from 0.01 – 5.93 tonCO_2/ton steel, whereas values for concrete range from 0.02 – 0.28 tonCO_2/ton. Likewise, the EEC's for steel range from 8.6 – 51 GJ/ton steel, whereas values for steel (no alloy) range from 8.3 – 50.7 GJ/ton. Concrete generally is much less emission intensive than steel for CO_2 and hence, is a lesser contributor to the sensitivity of embodied carbon. It can also be observed that while normal concrete EF and steel (no alloy) EEC contribute 9% each, steel EF and steel EEC contribute 78% and 62% respectively to the resulting uncertainty. This highlights the influence of the wider distribution range of steel (no alloy) EEC compared to normal concrete EF. Due to the wide distribution ranges and mass of steel, variations in steel EF's and EEC's have significantly more impact on the embodied energy and embodied carbon uncertainty even though there is normally more concrete than steel.

For TIO 1, normal concrete and steel are also major material components of the turbine with 575 tons and 141 tons respectively. However CFRP contributes considerably to the resulting uncertainty, second only to steel, while having a mass of 8.6 tons (1% of the turbine mass). This can be attributed to CFRP being very emission and energy intensive. The EF's for CFRP range from 11.2 – 86.3 tonCO_2/ton CFRP, compared to the steel EF range of 0.01 – 5.93 tonCO_2/ton steel. Similarly, the EEC's for CFRP range from 55 – 594 GJ/ton CFRP compared to the steel EEC range of 8.6 – 51 GJ/ton steel. Hence due to the wide distribution ranges in CFRP EF and EEC input factors, despite its minor mass contribution, CFRP has a considerable impact on the uncertainty of the embodied energy and embodied carbon. For TIO 2, the major material components are normal concrete and CFRP with 575 tons and 88.5 tons respectively. Despite being second in mass to steel, CFRP contributes 99% and 97% of the resulting uncertainty for embodied carbon and embodied energy respectively. This is attributed to its high emission intensity, energy intensity and wide distribution ranges. As a result, CFRP significantly impacts the uncertainty of the embodied energy and embodied carbon.

Normal concrete and steel are the major material components in TIO 3 with 575 and 144 tons respectively. The contribution of steel to the final resulting uncertainty is again attributed to the range of values of EF's and EEC's. Cast iron has a mass of 21 tons and EEC values ranging between 11.7 – 94.5 GJ/ton which could explain the lesser contribution of steel EEC to the resulting uncertainty for the embodied energy (66%) compared to the steel EF contribution for embodied carbon (81%). For TIO 4, the major material components are normal concrete with 575 tons and CFRP with 97 tons. CFRP contributes 98% and 97% of the resulting uncertainty for embodied carbon and embodied energy respectively. Again the sheer tonnage of CFRP combined with its high emission and energy intensity, and wide distribution ranges results in its significant contribution to the resulting uncertainty of the embodied energy and embodied carbon.

The intention of quantifying uncertainty with the HDS approach in this study is to provide more information for the decision making process. From the above case studies, it is assumed that the deterministic result is used for design scheme selection aiming to find an embodied carbon and embodied energy saving design. The design for the baseline turbine is already accepted since it is commercially available. If the design was rejected, in terms of embodied carbon, there would have been an about 85% probability (Fig. 3b) Enercon may have lost the chance to reduce carbon emissions with the design. Thus, it is a good design in terms of embodied carbon savings. In terms of embodied energy if the design was rejected, there would have been a 50% probability (Fig. 4b) Enercon may have lost the chance to reduce the primary energy consumed during manufacture. The TIO's proposed in this study are design concepts. Hence if the design for TIO 1 is accepted by a manufacturer, in terms of embodied carbon, there will be an about 85% probability (Fig. 5b) that the manufacturer may lose the chance to reduce carbon emissions with this design. Hence, it is not a good design in terms of embodied carbon savings. In terms of embodied energy, if the design is accepted, there will be a 40% (Fig. 6b) probability that the manufacturer may lose the chance to reduce the primary energy consumed. This design thus performs better in terms of embodied energy savings.

If the design for TIO 2 is accepted, results show that for embodied carbon, there is almost a 99% probability (Fig. 7b) the manufacturer may lose the chance to reduce carbon emissions hence making it a bad design. For embodied energy, results show that if this design is accepted, there is about a 20% probability (Fig. 8b) the manufacturer may lose the chance to reduce the primary energy consumed making it a good design in terms of embodied energy savings. The huge difference in the results, despite CFRP's contribution of 99% and 97% to the resulting uncertainty for embodied carbon and embodied energy, can be attributed to the differences in distribution ranges of steel (no alloy) and normal concrete EEC and EF input factors. EEC values of steel (no alloy) range from 8 – 51 GJ/ton compared to EF values of concrete that range from 0.02 – 0.28 tonCO_2/ton. This highlights how variations in EF and EEC values significantly affect results of embodied carbon and embodied energy LCA.

Results show that for embodied carbon if the design for TIO 3 is accepted, there will be a 15% probability (Fig. 9b) that the manufacturer may lose the chance to reduce carbon emissions with this design. It is therefore a good design in terms of embodied carbon savings. For embodied energy, results show that if this design is accepted, there is about a 65% probability (Fig. 10b) the manufacturer may lose the chance to reduce the primary energy consumed. This design therefore performs better in terms of embodied carbon savings. If the design for TIO 4 is accepted, in terms of embodied carbon, there would be about a 99% probability (Fig. 11b) that the manufacturer may lose the chance to reduce carbon emissions making it a bad design. For embodied energy, results show that if this design is accepted, the probability that the manufacturer may lose the chance to reduce the primary energy consumed is about 15% (Fig. 12b) making it a good design in terms of embodied energy savings. The difference in the results, despite CFRP's contribution of 98% and 97% to the resulting uncertainty for embodied carbon and embodied energy, could again be attributed to reasons described in TIO 2.

A direct comparison of this study with the few wind turbine LCA studies employing stochastic modelling to propagate uncertainty is difficult due to different assumptions which include scope of study, turbine capacities, background data and use of the pure DQI approach. For these reasons the wind turbine environmental impacts reported in the different studies vary. As there are no other wind turbine studies employing the HDS methodology, the closest study available in literature for comparison is Khan et al. (2005) for which the life cycle Global Warming Potential (95th percentile) of the wind turbine is 16.86 g CO_2 eq./kWh. From the results of the different case studies, more information was gained for decision making using the HDS approach compared to the DQI. The confidence level which is the important factor for decision making was observed and it can be seen that the DQI approach gave more conservative results, consistent with conclusions in Venkatesh et al.

(2010), Tan et al. (2002) and Lloyd and Ries (2007), which could lead to unreliable decisions. For example, the results for all the case studies showed the pure DQI approach giving a 50% probability making any decisions made using the pure DQI quite unreliable. Thus the HDS approach is a useful alternative for the evaluation of deterministic wind turbine embodied energy and embodied carbon LCA results when knowledge of the data uncertainties is required. The baseline wind turbine therefore performs best in terms of an embodied energy and embodied carbon saving scheme.

5.0 Conclusions

In this paper the competence of the HDS method in estimating data uncertainty in deterministic embodied carbon and embodied energy LCA results and its application to decision making is examined through case studies. In order to evaluate the reliability of the HDS method, first, embodied carbon and embodied energy results were estimated deterministically. Then for each case study, using DQI and HDS methods, the effect on uncertainty estimates for embodied energy and embodied carbon are investigated. In performing the uncertainty analysis, the reliability measures MRE and CV are considered. Using the results obtained the following conclusions are drawn.

Firstly, with respect to the use of both methods, the HDS approach demonstrated its effectiveness in evaluating deterministic 1.5 MW wind turbine embodied carbon and embodied energy results. MRE and CV results show the HDS far outperforms the DQI. In other words, a strong argument could be made to advocate for the use of the HDS over DQI when accuracy of the uncertainty estimate is paramount. Secondly, for the class of the problem at hand, similar conclusions can be drawn in terms of embodied energy and embodied carbon for all case studies. Uncertainty in the results largely depends on distribution ranges of the input parameters. This is magnified by the mass of the materials which result in the overall contributions to the uncertainty. Hence, it is shown that a strong relationship exists between material mass and input parameter distribution ranges. Thirdly, when comparing the different turbine designs based on the studied cases, the results were quite clear. With the performance improvements incorporated using the TIO's, the baseline turbine had the best embodied carbon and embodied energy performance. Therefore, when all the criteria are considered, the potential investor must decide whether the environmental benefits for a particular design are worth the investment.

It is important to note that the NREL baseline turbine design represents a composite of wind turbine technology available in 2002. Clearly, technology has changed since 2002 and these changes are not incorporated into the current analysis. Future studies may conduct uncertainty analysis using the HDS approach to analyse these technological changes in the development of newer wind turbines and other renewable technologies. This would be another excellent application for the HDS methodology.

References

A. Zamagni, P. Buttol, P.L. Porta, R. Buonamici, P. Masoni , J. Guinée, R. Heijungs, T. Ekvall, R. Bersani, A. Bieńkowska and U. Pretato (2008). “Critical review of the current research needs and limitations related to ISO-LCA practice”, Co-ordination Action for innovation in Life-Cycle Analysis for Sustainability*,* Italy

Alcorn, A. and P. Wood (1998). "New Zealand Building Materials Embodied Energy Coefficients Database Volume II–Coefficients." Centre for Building Performance Research, Victoria University of Wellington.

Ardente, F., et al. (2008). "Energy performances and life cycle assessment of an Italian wind farm." Renewable and Sustainable Energy Reviews 12(1): 200-217.

Arvesen, A. and E. G. Hertwich (2012). "Assessing the life cycle environmental impacts of wind power: A review of present knowledge and research needs." Renewable and Sustainable Energy Reviews 16(8): 5994-6006.

Aso, R. and W. M. Cheung (2015). "Towards greener horizontal-axis wind turbines: analysis of carbon emissions, energy and costs at the early design stage." Journal of Cleaner Production 87: 263-274.

Baird, G., et al. (1997). "The energy embodied in building materials-updated New Zealand coefficients and their significance."

Baum, A. W., et al. (2009). "The visible, sustainable farm: A comprehensive energy analysis of a Midwestern farm." Critical reviews in plant sciences 28(4): 218-239.

Canter, K. G., et al. (2002) Screening stochastic life cycle assessment inventory models. "The International Journal of Life Cycle Assessment", 7(1), 18-26.

Change, I. P. O. C. (2006). 2006 IPCC Guidelines for National Greenhouse Gas Inventories. Volume 3: Industrial Processes and Product Use. Chapter 4: Metal Industry Emissions

Chaouki Ghenai (2012). Life Cycle Analysis of Wind Turbine, Sustainable Development - Energy, Engineering and Technologies - Manufacturing and Environment, Prof. Chaouki Ghenai (Ed.), ISBN: 978-953-51-0165-9, InTech, Available from: http://www.intechopen.com/books/sustainable-development-energy-engineering-andtechnologies-manufacturing-and-environment/life-cycle-analysis-of-wind-turbine

Chen, G., et al. (2011). "Renewability of wind power in China: a case study of nonrenewable energy cost and greenhouse gas emission by a plant in Guangxi." Renewable and Sustainable Energy Reviews 15(5): 2322-2329.

Cohen, J., et al. (2008). "Technology improvement opportunities for low wind speed turbines and implications for cost of energy reduction." National Renewable Energy Laboratory, Golden, Colorado (US), Technical Report NREL/TP-500-41036.

Costanza, R. (1980). "Embodied energy and economic valuation." Science 210(4475): 1219-1224.

Davidsson, S., et al. (2012). "A review of life cycle assessments on wind energy systems." The International Journal of Life Cycle Assessment 17(6): 729-742.

Demir, N. and A. Taşkın (2013). "Life cycle assessment of wind turbines in Pınarbaşı-Kayseri." Journal of Cleaner Production 54: 253-263.

Douglas, C., et al. (2008). "Life cycle assessment of the Seagen marine current turbine." Proceedings of the Institution of Mechanical Engineers, Part M: Journal of Engineering for the Maritime Environment 222(1): 1-12.

Du, F., et al. (2012). "Life cycle analysis for water and wastewater pipe materials." Journal of Environmental Engineering 139(5): 703-711.

Duflou, J. R., et al. (2012). "Do fiber-reinforced polymer composites provide environmentally benign alternatives? A life-cycle-assessment-based study." Mrs Bulletin 37(04): 374-382.

Fernando, A. T. D. (2010). "Embodied energy analysis of New Zealand power generation systems. MSc Dissertation, University of Canterbury.

Fingersh, L. J., et al. (2006). Wind turbine design cost and scaling model, National Renewable Energy Laboratory Golden, CO.

Fleck, B. and M. Huot (2009). "Comparative life-cycle assessment of a small wind turbine for residential off-grid use." Renewable Energy 34(12): 2688-2696.

Garrett, P. and K. Rønde (2013). "Life cycle assessment of wind power: comprehensive results from a state-of-the-art approach." The International Journal of Life Cycle Assessment 18(1): 37-48.

Greening, B. and A. Azapagic (2013). "Environmental impacts of micro-wind turbines and their potential to contribute to UK climate change targets." Energy 59: 454-466.

Guezuraga, B., et al. (2012). "Life cycle assessment of two different 2 MW class wind turbines." Renewable Energy 37(1): 37-44.

Hammond, G. and C. Jones (2008). Inventory of carbon & energy: ICE, Sustainable Energy Research Team, Department of Mechanical Engineering, University of Bath, Bath, UK.

Hammond, G. and C. Jones (2011). "Inventory of Carbon & Energy Version 2.0 (ICE V2. 0)." Department of Mechanical Engineering, University of Bath, Bath, UK.

Hendrickson, T. P. and A. Horvath (2014). "A perspective on cost-effectiveness of greenhouse gas reduction solutions in water distribution systems." Environmental Research Letters 9(2): 024017.

Hill, N., et al. (2011). The role of GHG emissions from infrastructure construction, vehicle manufacturing, and ELVs in overall transport sector emissions, Task.

Howarth, J., et al. (2014). "Energy intensity and environmental analysis of mechanical recycling of carbon fibre composite." Journal of Cleaner Production 81: 46-50.

Huijbregts, M. A. (1998). "Application of uncertainty and variability in LCA." The International Journal of Life Cycle Assessment 3(5): 273-280.

Junnila, S. and A. Horvath (2003). "Life-cycle environmental effects of an office building." Journal of Infrastructure Systems 9(4): 157-166.

Kabir, M. R., et al. (2012). "Comparative life cycle energy, emission, and economic analysis of 100 kW nameplate wind power generation." Renewable Energy 37(1): 133-141.

Kelly, K., et al. (2014). "An energy and carbon life cycle assessment of industrial CHP (combined heat and power) in the context of a low carbon UK." Energy 77: 812-821.

Khan, F. I., et al. (2005). "Life cycle analysis of wind–fuel cell integrated system." Renewable Energy 30(2): 157-177.

Kirihara, T., et al. (2011). Demand and disposal forecast for carbon fibre by bottom-up approach. Proceedings of 18th International Conference of Composite Materials TH32.

Lantz, E., et al. (2012). IEA Wind Task 26: The Past and Future Cost of Wind Energy, Work Package 2, National Renewable Energy Laboratory (NREL), Golden, CO.

Lee, B., et al. (2011). "Embodied energy of building materials and green building rating systems—a case study for industrial halls." Sustainable Cities and Society 1(2): 67-71.

Lenzen, M. and C. Dey (2000). "Truncation error in embodied energy analyses of basic iron and steel products." Energy 25(6): 577-585.

Lenzen, M. and G. Treloar (2002). "Embodied energy in buildings: wood versus concrete—reply to Börjesson and Gustavsson." Energy policy 30(3): 249-255.

Lloyd, S. M. and R. Ries (2007). "Characterizing, Propagating, and Analyzing Uncertainty in Life-Cycle Assessment: A Survey of Quantitative Approaches." Journal of Industrial Ecology 11(1): 161-179.

Martínez, E., et al. (2009). "Life-cycle assessment of a 2-MW rated power wind turbine: CML method." The International Journal of Life Cycle Assessment 14(1): 52-63.

Martínez, E., et al. (2010). "LCA sensitivity analysis of a multi-megawatt wind turbine." Applied Energy 87(7): 2293-2303.

NETL (2010) NETL Life Cycle Inventory Data – Unit Process: Horizontal Turbine Main Frame, 1.5-6 MW Capacity, Manufacturing. U.S. Department of Energy, National Energy Technology Laboratory. Last Updated: November 2010 (version 01). www.netl.doe.gov/energy-analyses (http://www.netl.doe.gov/energy-analyses)

Norgate, T., et al. (2007). "Assessing the environmental impact of metal production processes." Journal of Cleaner Production 15(8): 838-848.

Oebels, K. B. and S. Pacca (2013). "Life cycle assessment of an onshore wind farm located at the northeastern coast of Brazil." Renewable Energy 53: 60-70.

Ortiz, O., et al. (2009). "Sustainability in the construction industry: A review of recent developments based on LCA." Construction and Building Materials 23(1): 28-39.

Padey, P., et al. (2012). "A simplified life cycle approach for assessing greenhouse gas emissions of wind electricity." Journal of Industrial Ecology 16(s1): S28-S38.

Papadopoulos, I. (2010). "Comparative analysis of electricity generating technologies with regards to environmental burdens". Ph.D Thesis, University of Bath, UK.

Pimenta, S. and S. T. Pinho (2011). "Recycling carbon fibre reinforced polymers for structural applications: Technology review and market outlook." Waste management 31(2): 378-392.

Rankine, R., et al. (2006). "Energy and carbon audit of a rooftop wind turbine." Proceedings of the Institution of Mechanical Engineers, Part A: Journal of Power and Energy 220(7): 643-654.

Rydh, C. J. and M. Sun (2005). "Life cycle inventory data for materials grouped according to environmental and material properties." Journal of Cleaner Production 13(13): 1258-1268.

Sefeedpari, P., et al. (2012). "Selecting energy efficient poultry egg producers: a fuzzy data envelopment analysis approach." International Journal of Applied Operational Research 2(2): 77-88.

Sharma, R., et al. (2013). "Conventional, hybrid and electric vehicles for Australian driving conditions. Part 2: Life cycle CO 2-e emissions." Transportation Research Part C: Emerging Technologies 28: 63-73.

Song, Y. S., et al. (2009). "Life cycle energy analysis of fiber-reinforced composites." Composites Part A: Applied Science and Manufacturing 40(8): 1257-1265.

Sugiyama, H., et al. (2005) Using Standard Statistics to Consider Uncertainty in Industry-Based Life Cycle Inventory Databases. "The International Journal of Life Cycle Assessment", 10(6), 399-405.

Tan, R. R., et al. (2002) Application of possibility theory in the life-cycle inventory assessment of biofuels. "International Journal of Energy Research", 26(8), 737-745.

TERI (2012). Final report - Life cycle analysis of transport modes (Volume II) New Delhi: The Energy and Resources Institute. 124pp. [Project code 2011UD02]

Tremeac, B. and F. Meunier (2009). "Life cycle analysis of 4.5 MW and 250W wind turbines." Renewable and Sustainable Energy Reviews 13(8): 2104-2110.

Uddin, M. S. and S. Kumar (2014). "Energy, emissions and environmental impact analysis of wind turbine using life cycle assessment technique." Journal of Cleaner Production 69: 153-164.

Venkatesh, A., et al. (2010). "Uncertainty analysis of life cycle greenhouse gas emissions from petroleum-based fuels and impacts on low carbon fuel policies." Environmental science & technology 45(1): 125-131.

Wang, E. and Z. Shen (2013) A hybrid Data Quality Indicator and statistical method for improving uncertainty analysis in LCA of complex system: application to the whole-building embodied energy analysis. "Journal of cleaner production", 43, 166-173.

Wang, Y. and T. Sun (2012) Life cycle assessment of CO2 emissions from wind power plants: Methodology and case studies. "Renewable Energy", 43, 30-36

Weidema, B. P. and M. S. Wesnæs (1996). "Data quality management for life cycle inventories—an example of using data quality indicators." Journal of Cleaner Production 4(3): 167-174.

Weinzettel, J., et al. (2009). "Life cycle assessment of a floating offshore wind turbine." Renewable Energy 34(3): 742-747.

Weitemeyer, S., et al. (2015). "Integration of Renewable Energy Sources in future power systems: The role of storage." Renewable Energy 75: 14-20.

World Wind Energy Association (2014). Available from: http://www.world-windenergy.info/ (Assessed 23/01/15)

Yang, Q., et al. (2013). "Environmental sustainability of wind power: an emergy analysis of a Chinese wind farm." Renewable and Sustainable Energy Reviews 25: 229-239.

Zhong, Z., et al. (2011). "LCAs of a polycrystalline photovoltaic module and a wind turbine." Renewable Energy 36(8): 2227-2237.

Zimmermann, T. (2013). "Parameterized tool for site specific LCAs of wind energy converters." The International Journal of Life Cycle Assessment 18(1): 49-60.

APPENDIX

	BOM			
	Material	Mass	Unit	Total
	Aluminium	99	kg	
	Fibre Glass	6564	kg	
	Epoxy resin	4548	kg	
	Hardener	1575	kg	
3 Blades	Polyamide	228	kg	
	Polyethene	684	kg	16152
	PVC foam	837	kg	
	PVC	393	kg	
	Paint	552	kg	
	Rubber	165	kg	
	Others (iron)	507	kg	
	Steel	144182	kg	
Tower	Galvanised steel	4695	kg	153094
	Paint	4217	kg	
	Copper	8988	kg	
	Steel sheet	17927	kg	

	Steel (no alloy)	13258	kg	
Generator	Steel (galvanised, low grade)	105	kg	40690
	Steel (alloy, high grade)	14	kg	
	Paint	150	kg	
	Others	248	kg	
	Steel (no alloy)	10780	kg	
	Steel (alloy, low grade)	9101	kg	
	Steel (galvanised, low grade)	1224	kg	
	Cast steel	3708	kg	
	Cast iron	21027	kg	
Rest of nacelle	Aluminium	127	kg	51591
	Copper	293	kg	
	Fibre glass	924	kg	
	Unsaturated polyester resin	2159	kg	
	Electronics	120	kg	
	Paint	504	kg	
	Others	1624	kg	
	Steel sheet	1300	kg	
	Steel (alloy, low grade)	927	kg	
	Steel (alloy, high grade)	630	kg	
	Steel (galvanised)	715	kg	
	Steel (for construction)	741	kg	
	Iron	1042	kg	
Grid Connection	Copper	6119	kg	27734
	PVC	747	kg	
	Gear oil	940	kg	
	Rest of electrics	1065	kg	
	Electronics	1283	kg	
	Light weight concrete	12000	kg	
	Others	225	kg	
	Normal concrete	575000	kg	
Deep foundations	Steel (construction)	26300	kg	614709
	Steel (no alloy)	13243	kg	
	PVC	166	kg	

Table 10: Material inputs to the Enercon E-66 wind turbine (Papadopoulos, 2010)